Preparation and Performance of Solid Oxide Fuel Cell Connector

Xuhan Li and Kening Sun

Abstract Lanthanum chromate ($LaCrO_3$) is a kind of ceramic bonding material in common use at present, in order to improve the phenomenon of poor sintering activity and conductivity, this article doped lanthanum chromate ($LaCrO_3$)-based materials with different elements and ratios to improve their performance. A series of $La_{0.8}Ca_{0.2}Cr_{1-x}Cu_xO_3$ ($x = 0.0, 0.1, 0.2, 0.3, 0.4, 0.5$) perovskite-type oxides were prepared by sol–gel method using $LaCrO_3$-based materials modified by Ca–Cu doping. After doping, the material has a series of advantages, such as coefficient of thermal expansion matching with electrolyte, and good chemical compatibility with other parts of the battery, good chemical stability in the reduction atmosphere, and high conductivity in the air and the reduction atmosphere, at 800 °C, the maximum conductivity of $La_{0.8}Ca_{0.2}Cr_{1-x}Cu_xO_3$ is 22.1 s cm^{-1} in air and 12.31 s cm^{-1} in H_2.

Keywords Connector · $LaCrO_3$ · Performance · Doping

1 Introduction

Solid oxide fuel cells (SOFCs) are a new type of energy conversion device, which can directly convert chemical energy into electrical energy. It has the advantages of simple system design, high energy efficiency, environmental friendliness, large-scale flexibility, and long life span, and is widely recognized as the green energy of the twenty-first century [1, 2]. SOFC is an all-solid structure. The key materials include electrolyte, cathode, anode, connecting material, and sealing material. The main function of electrolytes is to transport oxygen ions or protons, and the main function of electrodes is to conduct electrons and provide electrochemical reaction sites. The connecting material is mainly used for connecting the cathode and anode of adjacent batteries to form a battery stack [3, 4].

X. Li · K. Sun (✉)
School of Chemistry and Chemical Engineering, Beijing Institute of Technology, Beijing 100081, People's Republic of China
e-mail: 3020135344@qq.com

S. Yadav et al. (eds.), *Energy Power and Automation Engineering*, Lecture Notes in Electrical Engineering 1118, https://doi.org/10.1007/978-981-99-8878-5_14

If a single battery is used, there is a fatal drawback, which is that the output power is bound to be very low. So, we need to use battery packs, which means connecting multiple single batteries in series [5]. A connector needs to be added between the anode and cathode of two batteries. The function of the connecting material mainly includes two aspects: on the one hand, it should be separated physically to prevent the contact between the air electrode and the fuel gas and the contact between the fuel gas electrode and the oxidizing atmosphere; on the other hand, it acts as an electrical connection between one battery anode and another battery cathode [6, 7]. Therefore, the material requirements of the connection material are the most stringent. The successful development of competitive and inexpensive joining materials is critical to the eventual commercialization of SOFC. In general, a material that can become a good connector must have good conductivity, be dense enough to hinder the mixture of fuel and oxidant, and match the coefficient of thermal expansion of adjacent components (TEC), to reduce mechanical stress [8]. $LaCrO_3$-based materials are commonly used as ceramic linker materials, belonging to perovskite-type (ABO_3) composite oxides, which have the following excellent properties: (1) high electronic conductivity in oxidation and reduction atmosphere; (2) the compatibility of phase, microstructure, and thermal expansion with other components of fuel cell is good, which can meet the requirements of high temperature and corrosion resistance [9]. However, the main disadvantages of $LaCrO_3$ are its high melting point, difficulty in obtaining fully dense products, and poor sintering in air. In order to improve sintering ability and electrical conductivity, basic metals at La point or transition metals at Cr point have been studied [10–12].

In this work, $La_{0.8}Ca_{0.2}Cr_{1-x}Cu_xO_3 (x = 0.0, 0.1, 0.2, 0.3, 0.4, 0.5)$ doped with Cu and Ca was prepared by sol–gel method and Pechini citric acid method and sintered in air. The phase composition of the sintered powders was analyzed by X-ray diffraction (XRD). The coefficient of thermal expansion and electrical conductivity of the sintered powders were measured by thermal dilatometer and four-probe technique. The microstructures of the scanning electron microscope and sintered materials were observed by SEM, and the effects of different doping elements on the properties of the materials were studied.

2 Experimental

A series of $La_{0.8}Ca_{0.2}Cr_{1-x}Cu_xO_3 (x = 0.0, 0.1, 0.2, 0.3, 0.4, 0.5)$ perovskite powders doped with Ca and Cu (LCCCx, $0 \leq x \leq 0.5$) were prepared by sol–gel method. $La(NO_3)_3 \cdot 6H_2O$, anhydrous $CaCl_2$, $Cr(NO_3)_3 \cdot 9H_2O$ and $Cu(NO_3)_3 \cdot 3H_2O$ were stoichiometry and dissolved in deionized water. Citric acid was added to the solution, and the molar ratio of citric acid to total metal ions was 1.5:1. Then add ammonia to adjust the PH of the solution to 7. The PH-adjusted mixture is heated at 80 °C and stirred until most of the water in the solution evaporates to form a blue, transparent gel. It was then dried in an oven at 150 °C for 10 h in an air atmosphere to obtain a black dry gel precursor. To remove any residual carbon, the precursor was calcined

in a muffle furnace at 1000 °C for 5 h to obtain a brown-to-black powder (the color deepens with increasing Cu doping), La0.8Ca0.2Cr1–xCuxO$_3$ powder.

Using Brucker's D8 Advance X-ray powder diffractometer (XRD), at 40 kV and 20 mA, the samples were scanned by Cu–Kα Ray ($\lambda = 1.54051$å) at a scanning speed of 10° min^{-1} in the range of 10°–90° and characterized by phase structure analysis. The limiting slit is 1°, the transmitting slit is 1°, the receiving slit is 0.3°, and the sampling interval is 0.02°. The electrical conductivity of the samples was measured in the range of 300–800 °C by four-probe method in the air and hydrogen atmosphere, respectively, and the interval of 50 °C was measured once. The resistance of the sample was measured by the four-wire resistance mode of the digital multimeter, and the voltage between the two voltage lines was measured by the digital multimeter, the resistance value R between the sample voltage lines can be obtained. The conductivity of the sample can be calculated by the formula $\sigma = \mathrm{L/Sr}$. Where σ is the conductivity of the sample in units of S cm^{-1}, L is the length between the two voltage probes, and *S* is the cross-sectional area of the sample. The thermal expansion curve (TEC) was measured in the temperature range of 30–1000 °C by using a thermal expansion instrument. The microstructure of the prepared material and the micro-size and micro-morphology of the surface and cross-section of the joint material after co-firing with the anode support were observed by scanning electron microscope scanning electron microscope (SEM).

3 Result Analysis

This section mainly discusses various tests, characterization, and result analysis.

3.1 X-ray Diffraction a Series of LCCC$_x$ Powders Were Prepared by Sol–gel Method

The XRD patterns of LCCCx powders calcined at 1000 °C are shown in Fig. 1. As can be seen from the diagram, each proportion of the powder presents a distinct perovskite structure. However, when the doping amount of Cu is more than 0.3, a small number of impurity peaks appear. The software analysis shows that the impurity peaks are some copper compounds, which is because Cu is not completely doped into LCCCx powder during calcination, instead, other compounds form, which precipitate from the perovskite lattice during calcination.

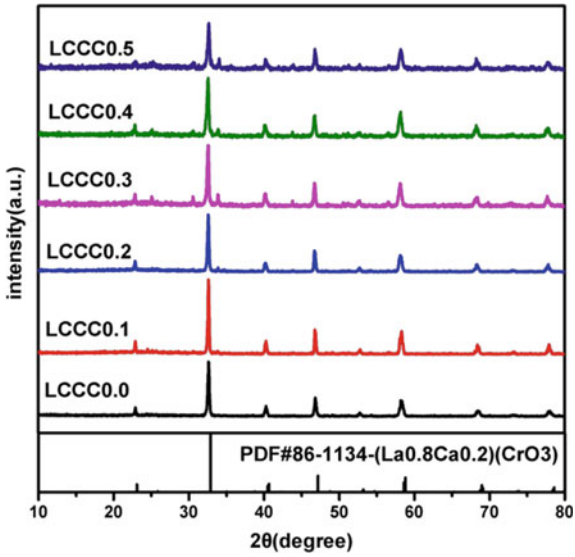

Fig. 1 XRD patterns of $La_{0.8}Ca_{0.2}Cr_{1-x}Cu_xO_3$ powder and comparison to PDF standard card

3.2 Scanning Electron Microscope (SEM) Characterization

The $LCCC_x$ powder was characterized by scanning electron microscopy powder was characterized by scanning electron microscope (SEM), to observe its morphological characteristics, as shown in Fig. 2. At the same time, $LCCC_x$ powder was prepared into screen-printing paste, which was coated on the anode support by screen-printing and sintered, and then characterized by scanning electron microscope scanning electron microscopy (SEM), as shown in Fig. 3. It can be seen from the figure that the particle size of $LCCC_x$ powder is relatively uniform, and the comparison of the surface electron microscope photographs of the powders with different proportions coated on the anode support after high temperature sintering by screen printing technology shows that, in addition to the undoped Cu and the powders with high doping content show poor sintered compactness, the other doped powders have good overall compactness. The reason is that when the Cu doping ratio is too high, the excess Cu is not completely doped into the $LCCC_x$ powder and precipitates, forming some other compounds, the impurity produced during sintering affects the densification degree of the junction surface. However, the overall results show that doping Cu into lanthanum chromate-based materials can improve the sintering activity to a certain extent, which is helpful to the sintering of materials to achieve higher density [13].

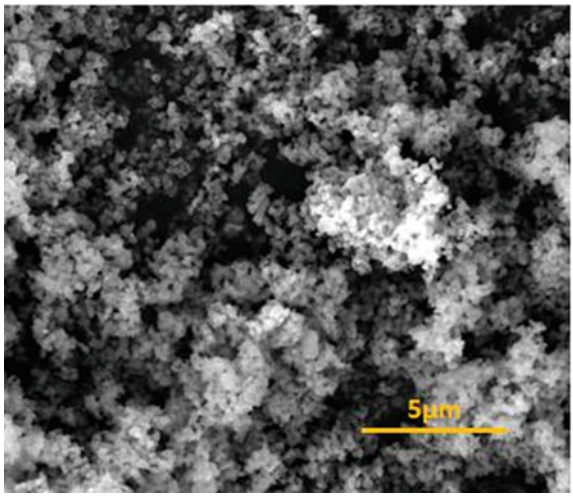

Fig. 2 SEM image of $La_{0.8}Ca_{0.2}Cr_{1-x}Cu_xO_3$ powder

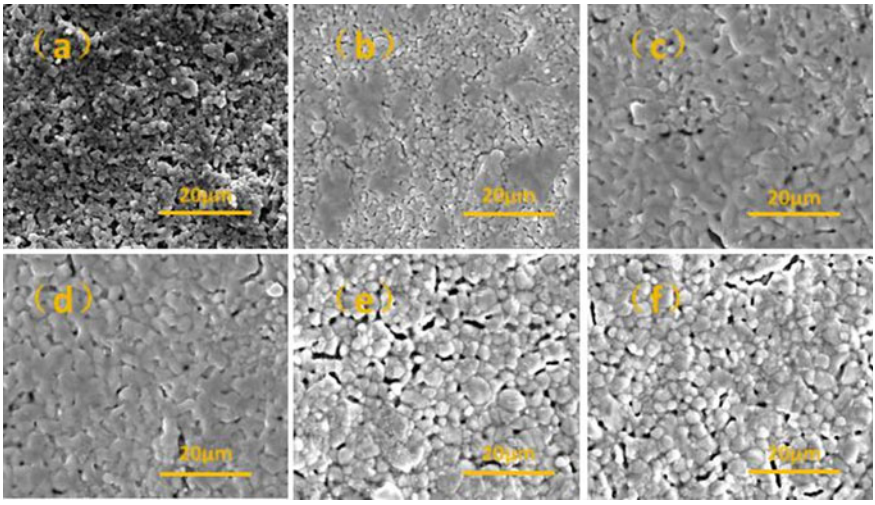

Fig. 3 SEM image of the doping ratios of $La_{0.8}Ca_{0.2}Cr_{1-x}Cu_xO_3$ powders after screen-printing sintering were, **a** 0.0, **b** 0.1, **c** 0.2, **d** 0.3, **e** 0.4, and **f** 0.5, respectively

3.3 Electrical Conductivity

Doping Cu with lanthanum chromate material will have an impact on conductivity. This article studies the changes in conductivity. Measure the conductivity of $LCCC_x$ under reduction and air conditions. Figure 4 shows the variation curve of $LCCC_x$ powder conductivity with temperature under air conditions. As shown in the figure, with the increase of temperature, the conductivity of the sample increases, and the

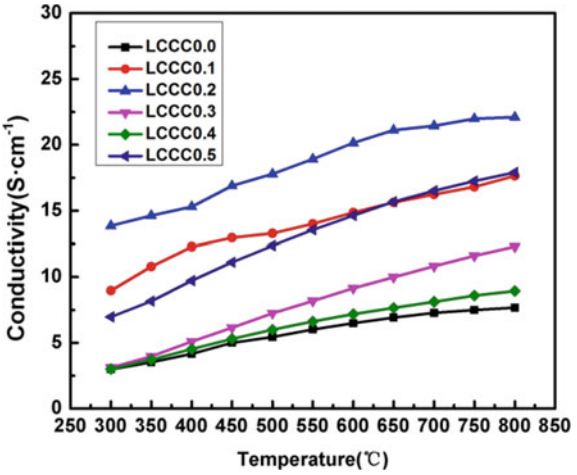

Fig. 4 $La_{0.8}Ca_{0.2}Cr_{1-x}Cu_xO_3$ conductivity in air atmosphere

more Cu doping, the conductivity curve of the sample shows a trend of first increasing and then decreasing [14]. However, the conductivity increases when the doping ratio of Cu is 0.5. According to the XRD analysis shown above, this is because some Cu precipitates in $LCCC_{0.5}$, which leads to the increase of conductivity. At 800 °C, the conductivity of $LCCC_{0.2}$ is the highest, up to 22.1 s cm^{-1}. The results show that the conductivity of lanthanum chromate-based materials is obviously improved after doping Cu, and the conductivity of lanthanum chromate-based materials is increased in a certain range.

The temperature dependence of conductivity of $LCCC_x$ samples in hydrogen atmosphere is shown in Fig. 5. Figure 5a is a function of conductivity with temperature in hydrogen and Fig. 5b is a curve of conductivity with Cu doping in hydrogen. As shown in the figure, under hydrogen conditions, the higher the temperature, the higher the conductivity of lanthanum chromate. In a reducing atmosphere, the conductivity of lanthanum chromate can be greatly improved by doping Cu. At the temperature of 800 °C, the conductivity of the samples without Cu doping is only 4.08 s cm^{-1} in the reduction atmosphere, but after Cu doping, the conductivity of the samples can reach more than ten s cm^{-1}. The electrical conductivity of Cu increased from 0 to 0.5 at first and then decreased in reducing atmosphere, and the electrical conductivity of $LCCC_{0.2}$ was the highest (12.31 s cm^{-1}).

Therefore, not only the increase of electrical conductivity was obviously improved by Cu doping in air atmosphere, but also the electrical conductivity of the samples changed from $LCCC_0$ 4.08 s cm^{-1} to $LCCC_{0.2}$ 12.31 s cm^{-1} in hydrogen atmosphere, the electrical conductivity is greatly improved. The reasonable conductivity of $LCCC_x$ in a dual atmosphere makes it a suitable connector material for flat tube solid oxide fuel cell.

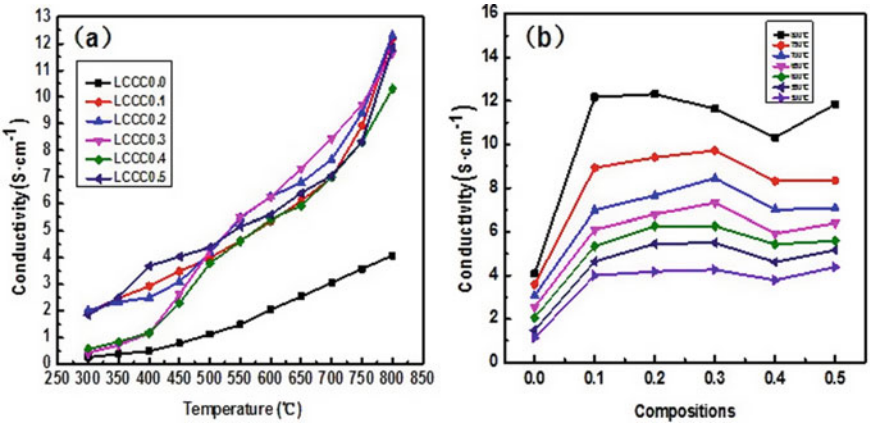

Fig. 5 $La_{0.8}Ca_{0.2}Cr_{1-x}Cu_xO_3$ conductivity in hydrogen atmosphere: **a** change with temperature; **b** change with Cu doping amount

3.4 *Study on Chemical Compatibility with Anode Powder and Electrolyte*

Because the connector material is in contact with the anode material NiO and the electrolyte material YSZ, in order to confirm the chemical compatibility of the connector with the anode and the electrolyte, the $LCCC_x$ powder was mixed with NiO and 8 mol% YSZ, respectively, at the mass ratio of 1:1, and then sintered at 1400 °C for 5 h.

Figure 6 shows the XRD spectra of the mixture of LCCCx and NIO, as well as a comparison to the XRD spectra of the mixture of NIO. Figure 7 shows the XRD spectra of $LCCC_x$ and YSZ mixture, and the comparison of the XRD patterns of the mixture with YSZ. From the observed XRD peak, there is no obvious formation of the second phase. So, under the normal calcination and working conditions of solid oxide fuel cell, the connector material $LCCC_x$ does not react with other components of the cell. The XRD spectrum of the calcined sample did not show any additional diffraction peaks, indicating that a second phase was not formed. Therefore, $LCCC_x$ is a cyclically stable connecting material.

3.5 *Thermal Shrinkage and Coefficient of Thermal Expansion*

The length of LCCCx strip samples was measured before and after calcination at 1400 °C. The thermal shrinkage of the $LCCC_x$ samples doped with Cu was all about 12%, the thermal shrinkage of the samples without Cu doping was only 5.77%.

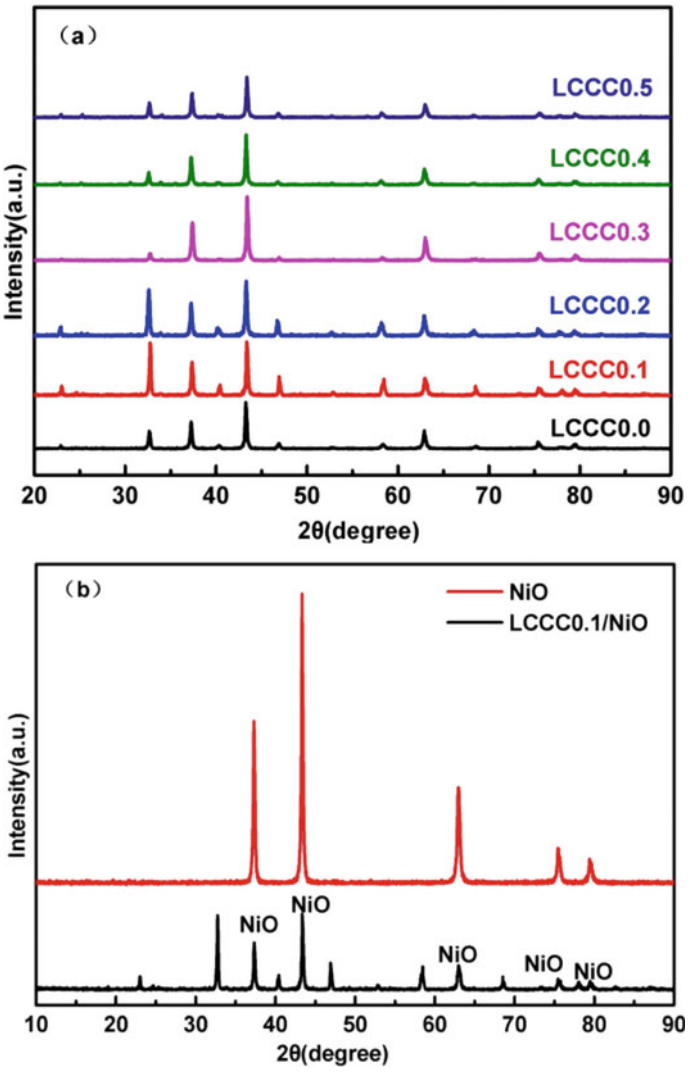

Fig. 6 **a** XRD patterns of the mixture of $LCCC_x$ with NiO (50:50 wt%) after 5 h of calcination at 1400 °C; **b** XRD comparisons of the mixture with NiO

At programmed temperature, the coefficient of thermal expansion of the connector material $LCCC_x$ was characterized by a thermal dilatometer and compared to other parts of the commonly used solid oxide fuel cell [15]. Between 30 °C and 1000 °C, the coefficient of thermal expansion of $LCCC_x$ closely matched the coefficient of thermal expansion of 8 mol% YSZ (10.6×10^{-6} K^{-1}), as shown in Fig. 7b. The TEC of $LCCC_0$ was 11.13×10^{-6} K^{-1}, still close to YSZ. The TEC of $LCCC_{0.1}$ is 10.58×10^{-6} K^{-1}, which is very similar to that of YSZ. The coefficients of thermal

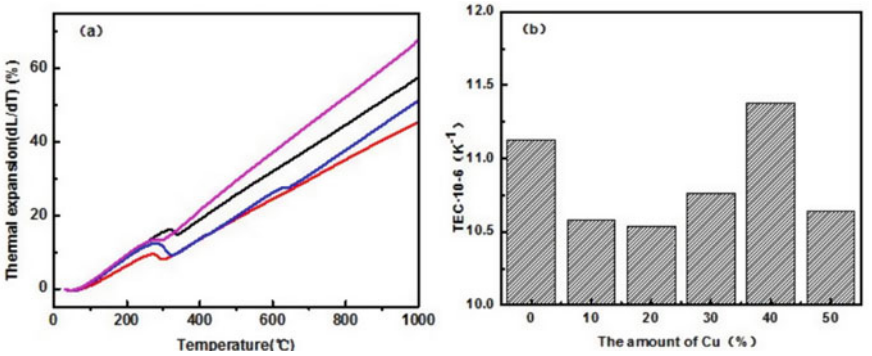

Fig. 7 **a** shows the thermal expansion curve of $La_{0.8}Ca_{0.2}Cr_{1-x}Cu_xO_3$ and **b** shows the thermal expansion curve of $La_{0.8}Ca_{0.2}Cr_{1-x}Cu_xO_3$ and the coefficient of thermal expansion curve (TEC) of $La_{0.8}Ca_{0.2}Cr_{1-x}Cu_xO_3$

expansion of $LCCC_{0.2}$–$LCCC_{0.5}$ were 10.54×10^{-6}, 10.76×10^{-6}, 11.38×10^{-6}, 10.64×10^{-6} K^{-1}, respectively, which were close to YSZ's TEC. It can be seen from the figure that Cu doping has a certain effect on TEC of lanthanum chromate, that is, with the increase of Cu doping amount, the coefficient of thermal expansion first decreases and then increases [16]. However, $LCCC_{0.5}$ contains impurities, which are different from their coefficient of thermal expansion and lead to the bending of the sample during the heating process, thus causing the difference in the coefficient of thermal expansion.

In addition, lanthanum chromate-based materials will change from orthorhombic system to trapezohexahedron, when the temperature rises to about 250–300 °C. Therefore, this phase transition process may occur during the heating of $LCCC_x$ samples. As shown in Fig. 7, it is obvious that there is an inflection point in the thermal expansion curve at about 300 °C. Although the material undergoes a phase transition around 300 °C, this does not affect the life of the solid oxide fuel cell, as the material is very close to YSZ's TEC [17, 18].

3.6 Study on the Stability in Reducing Atmosphere

The prepared $LCCC_x$ powder was placed in a tube furnace at 800 °C, and hydrogen was introduced into it to reduce it in hydrogen atmosphere for 10 h, then its XRD was tested. The XRD of reduced $LCCC_x$ powder is shown in Fig. 8. As can be seen from the diagram, there is no new impurity formation after 10 h of reduction, and $LCCC_x$ can keep a good perovskite structure. As a result, the $LCCC_x$ is stable for the duration of the solid oxide fuel cell, extending the battery's life to some extent [19].

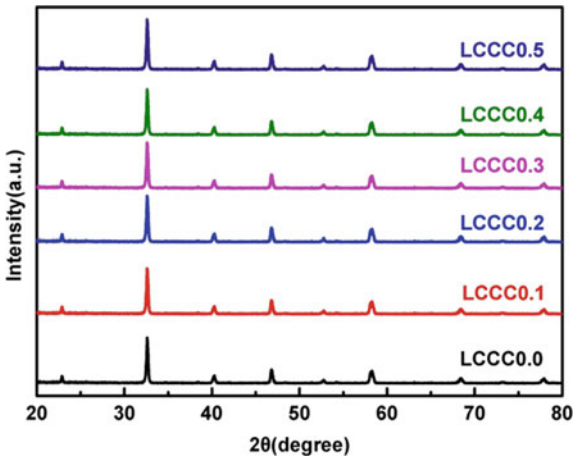

Fig. 8 XRD patterns of $La_{0.8}Ca_{0.2}Cr_{1-x}Cu_xO_3$ powders after 10 h reduction at 800 °C in hydrogen

4 Conclusion

A series of Ca and Cu doped lanthanum chromate ($La_{0.8}Ca_{0.2}Cr_{1-x}Cu_xO_3$($x = 0.0$, 0.1, 0.2, 0.3, 0.4, 0.5) ceramic perovskite powders were synthesized by sol–gel method, a series of characterizations were carried out. From the results, it can be seen that under air conditions, as Cu doping increases, the conductivity of the sample first increases and then decreases. But, when the atmosphere switches to hydrogen gas, the amount of Cu doping increases, and the conductivity first increases, then decreases. When the doping amount is increased again, the conductivity will increase. The electrical conductivity of $La_{0.8}Ca_{0.2}Cr_{0.8}Cu_{0.2}O_3$ is 22.1 s cm^{-1} at 800 °C in air atmosphere, and the electrical conductivity of $La_{0.8}Ca_{0.2}Cr_{0.8}Cu_{0.2}O_3$ increases greatly in hydrogen atmosphere, the conductivity of $La_{0.8}Ca_{0.2}Cr_{0.8}Cu_{0.2}O_3$ at 800 °C is 12.31 s cm^{-1}. The coefficient of thermal expansion of $La_{0.8}Ca_{0.2}Cr_{1-x}Cu_xO_3$($x = 0.0$, 0.1, 0.2, 0.3, 0.4, 0.5) is very close to the coefficient of thermal expansion of YSZ, and the coefficient of thermal expansion increases with the increase of Cu doping amount, in addition, the stability of the powder at high temperature (800 °C) and in reducing atmosphere was good, which met the requirements of the solid oxide fuel cell connector materials, and the powder had good chemical compatibility with NiO and YSZ, under high temperature conditions, it does not react with NiO and YSZ. Therefore, the properties of $La_{0.8}Ca_{0.2}Cr_{1-x}Cu_xO_3$($x = 0.0$, 0.1, 0.2, 0.3, 0.4, 0.5) powder are good, especially $La_{0.8}Ca_{0.2}Cr_{0.8}Cu_{0.2}O_3$ powder, very suitable for use as connector material.

References

1. Neelima M, Banerjee A, Gupta A, Omar S, Balani K (2015) Progress in material selection for solid oxide fuel cell technology: a review. Prog Mater Sci 72:141–337. https://doi.org/10.1016/j.pmatsci.2015.01.001
2. Grove WRXXIV (1966) On voltaic series and the combination of gases by platinum. Lond Edinb Dublin Philos Mag J Sci 14:127–130. https://doi.org/10.1080/14786443908649684
3. Gaugain J (1853) Note sur les signes electriques attribues au mouvement de la chaleur. CR Hebd Seances Acad Sci 37:82–84.https://doi.org/10.1016/S0035-3159(99)80026-9
4. Haber F, Moser A (1905) Das Generatorgas und das Kohlenelement. Z Elektrochem 11:593–609. https://doi.org/10.1002/bbpc.19050113603
5. Akashi T, Maruyama T, Goto T (2003) Transport of lanthanum ion and hole in $LaCrO_3$ determined by electrical conductivity measurements. Solid State Ionics 164:177–183. https://doi.org/10.1016/j.ssi.2003.08.050
6. Steele B (1995) Interfacial reactions associated with ceramic ion transport membranes. Solid State Ionics 75:157–165. https://doi.org/10.1016/0167-2738(94)00182-R
7. Lee GY, Song RH, Kim JH, Peck DH, Lim TH, Shul YG, Shin DR (2006) Properties of Cu, Ni, and V doped-$LaCrO_3$ interconnect materials prepared by pechini, ultrasonic spray pyrolysis and glycine nitrate processes for SOFC. J Electroceram 17:723–727. https://doi.org/10.1007/s10832-006-0473-1
8. Hilpert K, Steinbrech RW, Boroomand F, Wessel E, Meschke F, Zuev A, Teller O, Nickel H, Singheiser L (2003) Defect formation and mechanical stability of perovskites based on $LaCrO_3$ for solid oxide fuel cells (SOFC). J Eur Ceram Soc 23:3009–3020. https://doi.org/10.1016/S0955-2219(03)00097-9
9. Fabbri E, Pergolesi D, Traversa E (2010) Ionic conductivity in oxide heterostructures: the role of interfaces. Sci Technol Adv Mater 11:054503. https://doi.org/10.1088/1468-6996/11/5/054503
10. Barriocanal JG, Calzada AR, Arco MV, Sefrioui Z, Santamaria J (2008) Colossal ionic conductivity at interfaces of epitaxial ZrO_2: $Y_2O_3/SrTiO_3$ heterostructures. Science 321:676–680. https://doi.org/10.1126/science.1156393
11. Tarancón A (2009) Strategies for lowering solid oxide fuel cells operating temperature. Energies 2:1130–1150. https://doi.org/10.3390/en20401130
12. Guo X, Matei I, Lee JS, Maier J (2007) Ion conduction across nanosized CaF_2/BaF_2 multilayer heterostructures. Appl Phys Lett 91:103102. https://doi.org/10.1063/1.2779254
13. Zhu B (2009) Solid oxide fuel cell (SOFC) technical challenges and solutions from nano-aspects. Int J Energy Res 33:1126–1137. https://doi.org/10.1002/er.1600
14. Zhu B, Raza R, Abbas G, Singh M (2011) An electrolyte-free fuel cell constructed from one homogenous layer with mixed conductivity. Adv Funct Mater 21:2465–2469. https://doi.org/10.1002/adfm.201002471
15. Singhal SC (2002) Solid oxide fuel cells for stationary, mobile, and military applications. Solid State Ionics 152:405–410. https://doi.org/10.1016/S0167-2738(02)00349-1
16. Huang K, Singhal SC (2013) Cathode-supported tubular solid oxide fuel cell technology: a critical review. J Power Sources 237:84–97. https://doi.org/10.1016/j.jpowsour.2013.03.001
17. Kim JH, Song RH, Song KS, Hyun HS, Shin DR, Yokokawa H (2003) Fabrication and characteristics of anode-supported flat-tube solid oxide fuel cell. J Power Sources 122:138–143. https://doi.org/10.1016/S0378-7753(03)00431-2
18. Zhu WZ, Deevi SC (2003) Development of interconnect materials for solid oxide fuel cells. Mater Sci Eng A 348:227–243. https://doi.org/10.1016/S0921-5093(02)00736-0
19. Yang Z, Weil KS, Paxton DM, Stevenson JW (2003) Selection and evaluation of heat-resistant alloys for SOFC interconnect applications. J Electrochem Soc 150:A1188-1210. https://doi.org/10.1149/1.1595659